

# **Low-Field Permanent Magnet Halbach Array Project Report**

Summer Cherry, Adriano Cristaldi, Simran Fitzpatrick, Noah Markwell, Sam Miller, Dani

Topper, Logan Virgil

ES 1401-03 Intro to Engr Module 1 (2024F)

Dr. Charlotte Sappo

September 21, 2024

## **Table of Contents**

<b>I. Background</b>	<b>3</b>
<b>II. Proposal</b>	<b>4</b>
<b>III. Process</b>	<b>6</b>
<b>IV. Results and Evaluation</b>	<b>11</b>
<b>V. Follow Up</b>	<b>12</b>
<b>VI. References</b>	<b>13</b>

## Background

(N)MRI, or (nuclear) magnetic resonance imaging, employs magnets to take noninvasive, cross-sectional anatomical images. The magnetic field produced by MRI forces protons in tissue to align with the field, 'exciting' them. As the protons 'relax,' or return to their original state, the MRI spectrometers detect the change in energy and relaxation time, from which the chemical nature of the tissue is able to be determined.<sup>1 2</sup> MRI is used to investigate soft tissue such as the brain, because of soft tissue's high water content.<sup>3</sup> MRI can also distinguish between fatty and water-based tissues in the human body, with T1-weighted images including fatty tissues, and T2-weighted images including both fatty and water-based tissues.<sup>4</sup> T1-weighted images generally include soft-tissue anatomy and fat, and are useful for diagnosing fat-containing masses. T2-weighted images complement T1-weighted images and show fluid and abnormalities such as tumors, inflammation, and trauma.<sup>5</sup> T1-weighted images obtained from low-field systems are favorable because the difference in T1 values of different tissues are larger, resulting in images with higher contrast between types of tissues.<sup>6</sup>

The magnet built for this project is a low-field system, which is advantageous for several reasons. Low-field magnets have lower siting and building costs because they do not require shielding (copper shield around high-field MRI), and need weaker magnets than their high-field

---

<sup>1</sup>National Institute of Biomedical Imaging and Bioengineering |. (n.d.). Magnetic Resonance Imaging (MRI). National Institute of Biomedical Imaging and Bioengineering |. Retrieved September 21, 2024, from <https://www.nibib.nih.gov/science-education/science-topics/magnetic-resonance-imaging-mri>

<sup>2</sup>Lloyd, G. (2017, September). MRI interpretation - MRI signal production. Radiology Masterclass -. Retrieved September 21, 2024, from [https://www.radiologymasterclass.co.uk/tutorials/mri/mri\\_signal](https://www.radiologymasterclass.co.uk/tutorials/mri/mri_signal)

<sup>3</sup>NCBI. (2021, February 25). T1-weighted and T2-weighted MRI image synthesis with convolutional generative adversarial networks. NCBI. Retrieved September 21, 2024, from <https://www.ncbi.nlm.nih.gov/pmc/articles/PMC8086713/>

<sup>4</sup>Lloyd, G. (2017, September). MRI interpretation - T1 v T2 images. Radiology Masterclass -. Retrieved September 21, 2024, from [https://www.radiologymasterclass.co.uk/tutorials/mri/t1\\_and\\_t2\\_images](https://www.radiologymasterclass.co.uk/tutorials/mri/t1_and_t2_images)

<sup>5</sup>Mafraji, M. A. (2023, November). Magnetic Resonance Imaging - Magnetic Resonance Imaging. Merck Manuals. Retrieved September 21, 2024, from <https://www.merckmanuals.com/professional/special-subjects/principles-of-radiologic-imaging/magnetic-resonance-imaging>

<sup>6</sup>ES 1401-03 Intro to Engr Module 1 (2024F) Assignment 1: Engineering Designs and Solutions Takeaways

counterparts. Low-field MRIs are lighter than high-field MRIs and need less space. They also use less energy and do not require cryogen or its accompanying pipe. Low-field MRI has less magnetic susceptibility, which makes scanned materials less prone to being altered by the magnetic field. Gradient noise is also lower due to reduced Lorentz forces, which is the force on a charged particle as it moves through an electromagnetic field.<sup>7</sup>

The magnet is a Halbach Array made from permanent magnets. This type of magnet does not necessitate a power source, cooling system, field lock system, and is safer to build. It also does not require passive or active shimming to make the magnetic field more homogenous.<sup>8</sup> 50 N52 magnets (higher energy density) and 50 N42 magnets (lower energy density) were used. The goal was to maximize the magnetic field strength ( $B_0 \approx 45\text{mT}$ ) produced by the magnet while creating the most homogenous field possible. The magnet also had to contain the other components of the MRI (gradient, coil, phantom) and be able to contain a diameter of scanning volume (DSV) of at least 3 inches, or the size of the phantom.

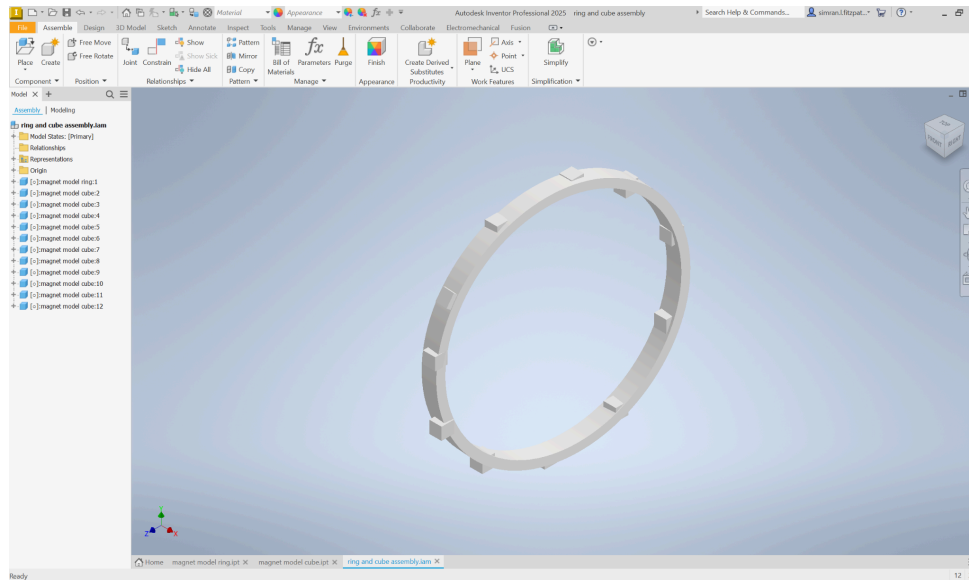
## **Proposal**

The initial proposal primarily served to communicate the dimensions of the magnet to other groups. The original proposal was an array of 50 magnets of the same strength (either N52 or N42), with 5 rings of 10 magnets each. The proposed inner diameter of the magnet was 6.5 inches, and the outer diameter was 7 inches, producing a 0.5 inch thick ring.

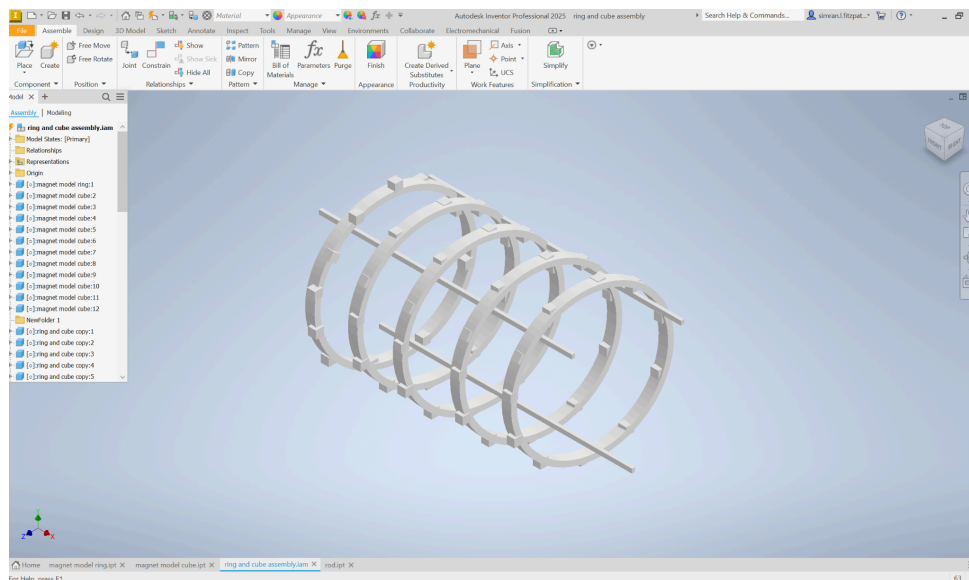
---

<sup>7</sup>Whitesides Research Group. (2024). Lorentz Effects. Whitesides Research Group. Retrieved September 21, 2024, from <https://www.gmwgroup.harvard.edu/lorenz-effects>

<sup>8</sup>ELSTER LLC. (2024). Magnetic shimming. Questions and Answers in MRI. Retrieved September 21, 2024, from <https://mriquestions.com/why-shimming.html>



*1: Initial design of one ring of a Halbach Array*



*2: Proposal for threading magnet rings together*

Although the proposal successfully outlined the general dimensions and shape of the Halbach array, as well as an idea of threading the rings of the Halbach array together, the initial proposal was not optimized for field strength or homogeneity. Upon optimizing the field strength and homogeneity, it was determined that 2 rings of magnets (inner and outer) were necessary,

and all 100 magnets needed to be used together to produce a sufficient  $B_0$ . The rings were also spaced very close together to increase the field strength over a smaller DSV.

## Process

First, the magnetic field was simulated using code from the Leiden University Medical Center, whose code is “an implementation of a genetic algorithm to optimize the homogeneity of a Halbach array by varying the ring diameters along the length of the Halbach cylinder.”<sup>9</sup> The code was modified to determine the optimal number of inner and outer rings, the number of magnets in each ring, ring separation (meters), and DSV (meters).

```
24
25 if __name__ == "__main__":
26
27     innerRingRadii = np.array([148, 154, 159, 165, 171, 177, 183, 189, 195, 201])*1e-3
28     innerNumMagnets = np.array([50, 52, 54, 56, 58, 60, 62, 64, 66, 68])
29
30     outerRingRadii = innerRingRadii + 12.75*1e-3 #0.5in separation (allows rings to fit together)
31     outerNumMagnets = innerNumMagnets + 6
32
33     resolution = 5
34     numRings = 10
35     ringSep = 0.0015875 #.125 inches to meters 0.5 depth minus 3/8 inch magnet
36     magnetLength = (numRings - 1) * ringSep
37     ringPositions = np.linspace(-magnetLength/2, magnetLength/2, numRings)
38
39
40     #population
41     popSim = 10000
42     maxGeneration = 100
43
44     DSV = 78 * 1e-3
45
46     #####
47     #####                                #####
48     #####                                Create spherical mask #####
49     #####                                #####
50     #####
51
```

### 3: Constraints in the Leiden University Medical Center Halbach Optimization Code

The first lines edited were line 27 and 28, where magnets were removed from the hard-coding of the array; and line 42, where the number of iterations was decreased to reduce the

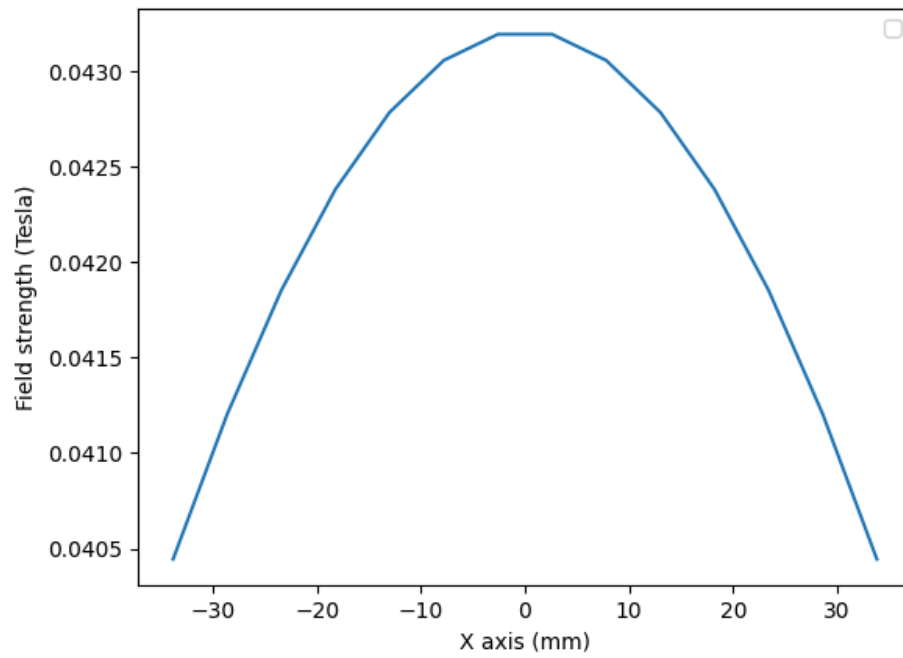
---

<sup>9</sup>2024 GitHub, Inc LUMC-LowFieldMRI

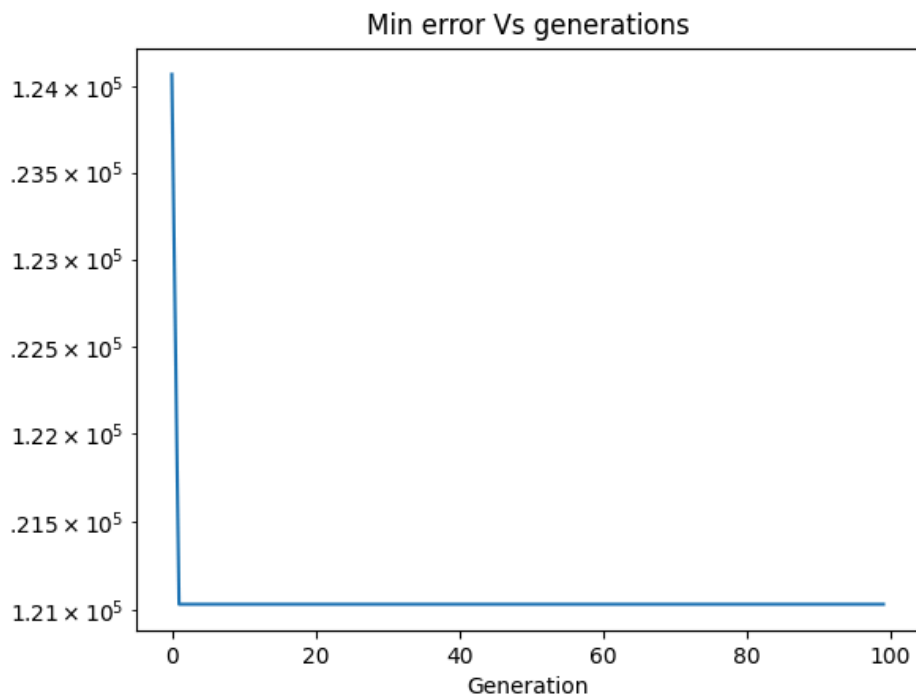
running time of the code. From there, the following constraints were edited to test which properties produced the highest  $B_0$  and most homogenous field: the difference between the radius of the inner and outer ring (line 30), the difference between the number of magnets in the inner and outer ring (line 31), the number of rings (line 34), the separation between rings (line 35), and the diameter of spherical volume (line 44). After running the code 23 times with varying parameters, it was determined that the highest  $B_0$  and a satisfactory homogeneity was created with:

- A smaller distance between the inner and outer ring
- A larger difference in the number of magnets between the inner and outer rings, with the outer ring having more magnets
- A higher number of rings
- A smaller ring separation
- A smaller DSV

The parameters were changed to correspond to these rules within the given constraints. The distance between the inner and outer ring was reduced to 0.5 inches to minimize the separation while allowing the inner ring to fit within the outer ring. The difference in the number of magnets between the inner and outer rings was optimized using a system of equations, which resulted in 66 outer magnets and 35 inner magnets across 5 rings, resulting in 7 magnets on an inner ring and 13 magnets on an outer ring. This increased the difference in the number of magnets between inner and outer rings to 6. The number of rings was increased to 10, including 5 inner rings and 5 outer rings. The ring separation was squeezed to 1/16 of an inch. The DSV was reduced to 78mm, or 3.07 inches, barely covering the required DSV of 3 inches or 76mm. When these parameters were inputted, the following results were produced:

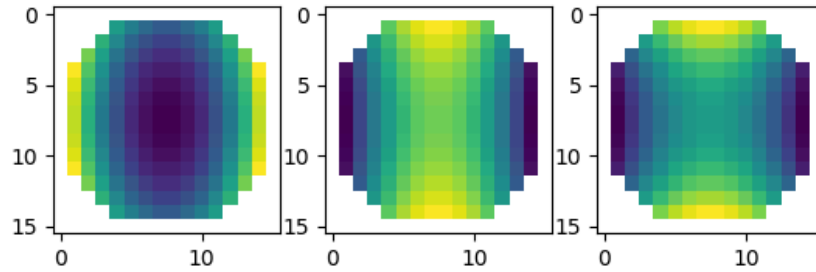


4: Field Strength over DSV



5: Min error vs. Generations



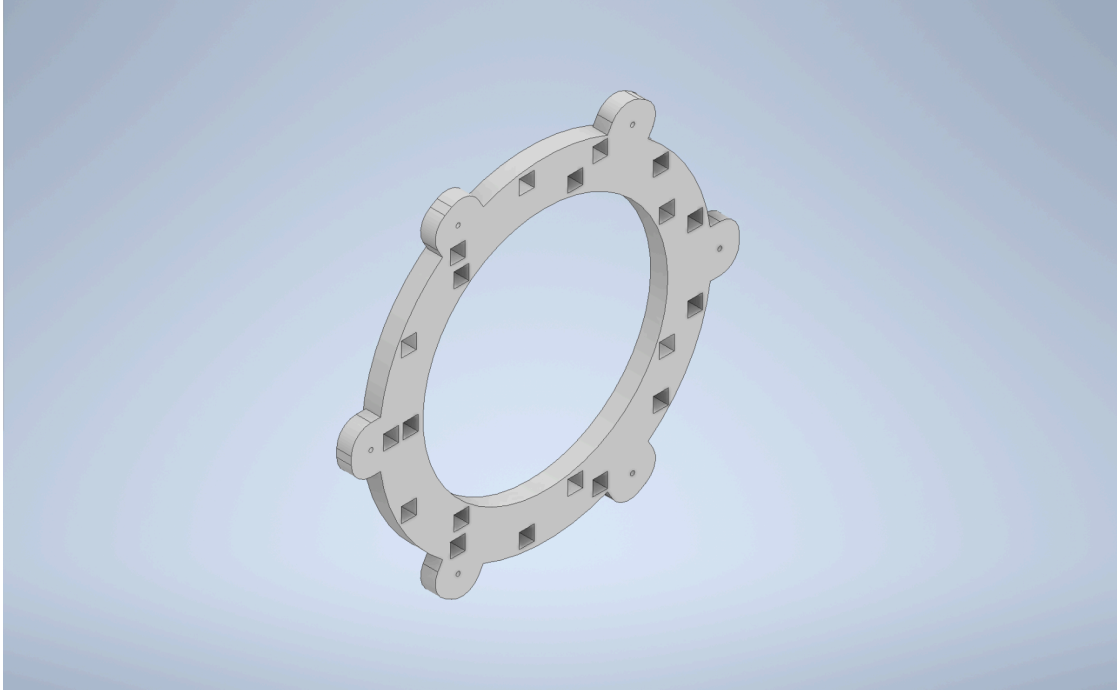


### *6: Homogeneity*

The parameters produced a  $B_0$  of 43mT, just below the goal of 45mT. The minimum error vs. generations of the simulation was reduced throughout the iteration process, which is expected. The homogeneity of the field is adequate, and could be improved by narrowing the rings into more of an oval shape rather than a perfectly circular ring of magnets.

One major overlook during this process was the failure to account for the strength of the individual magnets. The parameters inputted did not adjust the field strength of the magnets from the default code, and also failed to account for the difference in field strength between types of magnets.

The parameters generated by the simulation were then used to create a CAD model of the Halbach array. Initially, the model was 2 separate rings that had to be clipped together, but was updated into one combined design with an inner diameter of 6.25 inches, pictured below:



*7: The final CAD model with an inner diameter of 6.25in.*

5 of the above combined inner-outer rings were 3D printed. The rings were printed from plastic, which is non conductive and would not interfere with the magnetic field. The spaces meant to hold the magnets were whittled out, and the north and south pole of each magnet were marked and inserted with the north side facing away from the center of each ring. Once each ring was filled with magnets, they were attached together with threads in a team effort and secured in place with washers.

## **Results and Evaluation**

An image has not yet been produced, but a Halbach Array fitting the size and resource constraints has been successfully assembled and produces a magnetic field, evidenced by its effect on magnets and other metal objects (i.e. scissors and phones) being inserted into the array. The success of this project was that it resulted in a Halbach Array with the constraints given and

producing a magnetic field. However, many things could have been done differently to make a more accurate and effective magnet.

Primarily, the field strengths of each individual magnet were not simulated. This definitely resulted in differences between the simulated  $B_0$  and homogeneity of the magnet, and what was actually produced. This could have either a negative or a positive effect on the  $B_0$  and homogeneity: if the default code used magnets that had a lower field strength than what was used in the construction of the magnet, then the actual  $B_0$  and homogeneity could be better than what was simulated. However, the opposite is true as well: if the default code used higher-strength magnets than what were available in construction, the  $B_0$  and homogeneity are likely worse in actuality.

In addition, there were discrepancies in the magnets used in the inner and outer rings. To account for the difference in field strength, lower-strength N42 magnets were used in the inner rings and higher-strength N52 magnets were used in the outer rings to attempt to normalize the field in the DSV. However, this was also contrary to the simulation. Some magnets were also not glued in due to time constraints, further weakening the homogeneity of the magnetic field.

The magnet's narrow size appeared to be a flaw because the magnet was much narrower than the other components once assembled. However, although the magnet was much narrower than the gradient and coil components, the diameter was wide enough to fit around all other components. Also, the magnet had been optimized to have a DSV of above 3 inches, so it theoretically could accommodate the 3 in<sup>3</sup> phantom being scanned. The magnet's parameters were "squeezed" to create the highest  $B_0$  field possible, and producing a wider magnet was not possible with the given constraints. Another result of this "squeezing" was that the ring

separation was only 1/16 inches, making it difficult to thread the rings together because the magnets were very close to each other and the rings repelled each other.

### **Follow up**

In further simulation, the actual magnet strengths will be inputted into the Leiden University Medical Center code to see what the resulting  $B_0$  is, which will be more accurate to the magnet produced. Once an image is produced, the efficacy of the low-field Halbach array can be evaluated. If a satisfactory image is produced, it is encouraging for increased low-field MRI accessibility.

## References

- ELSTER LLC. (2024). *Magnetic shimming*. Questions and Answers in MRI. Retrieved September 21, 2024, from <https://mriquestions.com/why-shimming.html>
- Lloyd, G. (2017, September). *MRI interpretation - MRI signal production*. Radiology Masterclass -. Retrieved September 21, 2024, from [https://www.radiologymasterclass.co.uk/tutorials/mri/mri\\_signal](https://www.radiologymasterclass.co.uk/tutorials/mri/mri_signal)
- Lloyd, G. (2017, September). *MRI interpretation - T1 v T2 images*. Radiology Masterclass -. Retrieved September 21, 2024, from [https://www.radiologymasterclass.co.uk/tutorials/mri/t1\\_and\\_t2\\_images](https://www.radiologymasterclass.co.uk/tutorials/mri/t1_and_t2_images)
- Mafraji, M. A. (2023, November). *Magnetic Resonance Imaging - Magnetic Resonance Imaging*. Merck Manuals. Retrieved September 21, 2024, from <https://www.merckmanuals.com/professional/special-subjects/principles-of-radiologic-imaging/magnetic-resonance-imaging>
- National Institute of Biomedical Imaging and Bioengineering |. (n.d.). *Magnetic Resonance Imaging (MRI)*. National Institute of Biomedical Imaging and Bioengineering |. Retrieved September 21, 2024, from <https://www.nibib.nih.gov/science-education/science-topics/magnetic-resonance-imaging-mri>
- NCBI. (2021, February 25). *T1-weighted and T2-weighted MRI image synthesis with convolutional generative adversarial networks*. NCBI. Retrieved September 21, 2024, from <https://www.ncbi.nlm.nih.gov/pmc/articles/PMC8086713/>
- Whitesides Research Group. (2024). *Lorentz Effects*. Whitesides Research Group. Retrieved September 21, 2024, from <https://www.gmwgroup.harvard.edu/lorenz-effects>